JOURNAL OF PROPULSION AND POWER
Vol. 22, No. 1, January–February 2006

Transpiration Cooling Experiment for Scramjet Engine Combustion Chamber by High Heat Fluxes

Kyo D. Song*
Norfolk State University, Norfolk, Virginia 23504
and
Sang H. Choi† and Stephen J. Scotti‡
NASA Langley Research Center, Hampton, Virginia 23681

A transpiration cooling experiment using an optical heating method that provided a heat flux as high as 234 W/cm^2 on the surface of specimen for a scramjet engine was performed. In this experiment, 19-mm-diam sintered, powdered, stainless-steel tubes and a 25-mm square cross-sectional tube of perforated Inconel tube were used to investigate transpiration cooling effectiveness. The cooling effectiveness by transpiration for each specimen was measured and analyzed. As a result, the transpiration cooling mechanism appeared to be a promising approach to remove a large amount of heat from the engine wall. A preliminary analysis of the transpiration cooling mechanism and a scaling conversion study that translates the results from helium tests into the case when a hydrogen medium is used are included.

Nomenclature

C	=	conversion constant, 1.33×10^4
C_p	=	specific heat capacity
$\dot{m}$	=	mass flux
P	=	pressure
$\dot{Q}$	=	heat flux
$T_{g\text{-in}}$	=	gas temperature entering
$T_{g\text{-out}}$	=	gas temperature existing
t	=	thickness
V	=	velocity
η	=	effectiveness
κ	=	permeability
μ	=	viscosity

Introduction

THE peak heating rate generated in a combustion chamber of a scramjet engine on a hypersonic vehicle varies from 120 to 2344 W/cm^2 (2000 Btu/ft^{2}s) (Ref. 1) depending on location as shown in Fig. 1. Such high heating rates created during a hypersonic flight pose a significant problem for the development of such vehicles.

Figure 2 shows the estimated heat loads within a scramjet engine at a Mach 15 flight condition.[1] The most extreme heat loads are created within the engine combustor, and these conditions impose the most difficult requirements to accommodate for the thermal-structural design of the engine. The passive, ablative thermal protection systems that have been studied for many years for single-use reentry vehicles are not appropriate for this application. The thermal protection system for a scramjet engine must differ from reentry vehicles because of the reusability requirement, maintenance of precise geometric contours, and incorporation of a hydrogen propellant.

Heat dissipation mechanisms are generally adopted according to heating loads, such as the employments of ablative materials, regenerative cooling using hydrogen fuel, gas film or transpiration cooling, or active heat-pipe cooling.[1–5] The ablative heat dissipation mechanism appears inapplicable for continuous and repeated operation of hypersonic vehicles because of significant ablative loss of combustor materials. Regenerative cooling is marginal because it poses significant materials' coating and system challenges due to large induced efficiency penalties in the hypersonic vehicle. However, the gas bleeding or transpiration cooling method appears attractive because the coolant bled through pores of wall panels removes the heat absorbed by the combustor wall and also effectively restructures a cool boundary layer that prevents the combustor wall from direct contact of combustion gas. The restructured cool boundary layer may alleviate convective heating by shielding the wall from hot combustion gases. If the transpirant adopted for cooling is also a propellant such as hydrogen, the injection of propellant into the scramjet combustion chamber through the combustor wall may be beneficial for better mixing of propellant in a supersonic combustion process, but it may also increase the amount of heat to the combustor wall due to the local burning near the wall.

To ensure structural robustness of scramjet engine components for long-duration exposure in the high heat flux ranging up to 120 W/cm^2, several materials for a transpiration cooling system have been tested in the laboratory. The combustion chamber of a scramjet engine requires a very effective heat dissipation mechanism to sustain such a high heating load. This research focused on the transpiration cooling mechanism that appears to be a promising approach to remove a large amount of heat from the engine wall. In a scramjet, a tremendous heat flux (average 535 W/cm^2) is generated from a supersonic combustion process of cryogenic hydrogen fuel. As a result, the engine wall of a scramjet is exposed to such a high heating load. To alleviate an unbearably high heating load, the transpiration cooling mechanism was adopted for an experimental investigation to determine its cooling effectiveness and its capability to shield the combustor wall from hot combustion gases. Thus, a radiative heating technique was adopted in the experiment to find the transpiration cooling effect without regard to the transpiration boundary layer.

In this experiment, an argon arc lamp that generates emission spectra at a 6500 K color temperature was used. The emission of argon arc that was measured with an optical multichannel analyzer is similar to a solar spectrum as shown in Fig. 3. The argon arc has a cylindrical volume 15 cm long and is 1.1 cm in diameter. The system generates a 60-kW optical power output.

This optical output power is generated from a linear argon arc tube that is located at a focal line within an elliptic reflector cavity

Received 4 June 2004; revision received 17 February 2005; accepted for publication 26 February 2005.

*Professor, Department of Engineering, Center for Materials Research; ksong@nsu.edu.
†Senior Research Scientist, Mail Stop 188 D. Associate Fellow AIAA.
‡Senior Research Engineer, Mail Stop 396. Member AIAA.

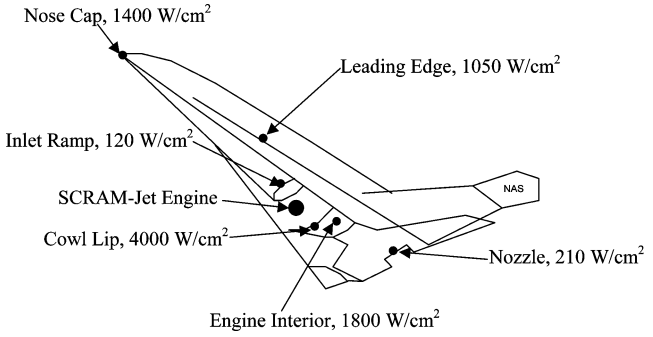

Fig. 1 Hypersonic vehicle aero/thermal environment.[1]

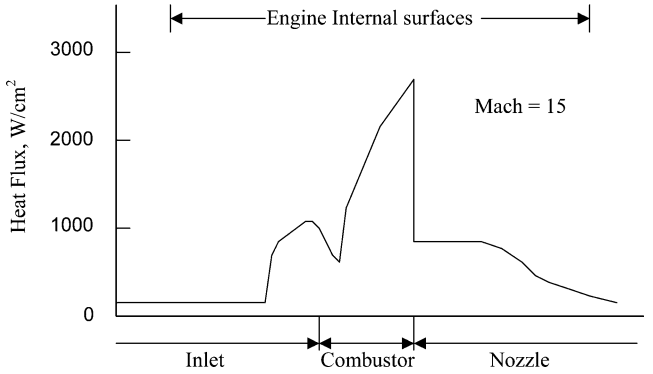

Fig. 2 Typical heat flux distribution in scramjet engine.[1]

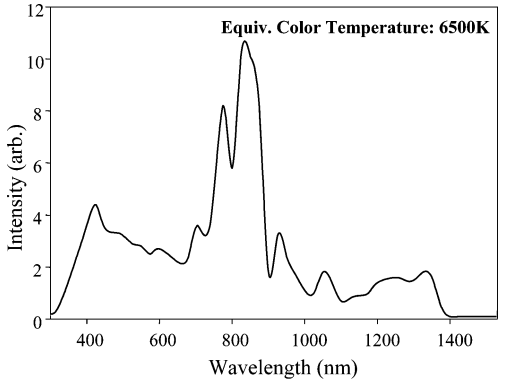

Fig. 3 Spectral energy distribution of argon arc lamp.

and is collected and focused at the other focal line where a test specimen is placed. The collected optical beam is, thus, uniform over the length of and around the body of a specimen. The uniform heat flux concentrated on a focal line of the elliptic reflector cavity is so intense that the temperature of a specimen rises immediately to a targeted level. Such a heating rate is unavailable from conventional heating sources.

Experiment

The setup for a transpiration cooling experiment is shown in Fig. 4. An argon arc lamp that generates a 60-kW optical power output from a 150-kW electrical input power was the heating source for the transpiration cooling experiment (TCE). The test bench for the TCE consists of an arc lamp, an elliptical reflector cavity, a test section at where a specimen is placed for the exposure to intense light, three pressure gauges, two thermocouples, an infrared thermometer, and two flow meters adopted for control and measurement of physical parameters as shown in Fig. 4. The radiant emission from the arc lamp is focused on a specimen to simulate the radiant heat flux in the scram-jet combustor. To collect and concentrate effectively optical power from the arc lamp onto the specimen, an elliptical reflector conduit is used. The arc lamp is placed at a focal line of the elliptical reflector conduit and the specimen at the other focal line as shown in Fig. 5. Once a specimen is placed on the focal line, the reflective side plates seal the elliptical reflector conduit to contain optical beam energy within the cavity.

Two types of test specimen were prepared: stainless-steel tubes 19 mm in diameter and 15 cm long and a middle portion consisting of sintered 1.5-, 3-, and 5-μm particulates[6] and a square cross-sectional tube (2.54 by 2.54 cm and 15 cm long) that was fabricated with multilayers of thin and perforated stainless plates[7] as shown in Fig. 6. All specimens have two thermocouples imbedded at both the inside and outside surfaces of their middle portion to measure the surface temperatures. The thermocouple wires run through the inside of the tube. An additional thermocouple was used to measure gas temperature downstream of the flow. A thermal radiometer (infrared thermometer) was used for measuring the outside temperatures of the specimen. In general, the thermophysical characteristics of porous specimens were determined by a thermal imaging system, thermocouples, flowmeters with controller, pressure transducers, and an anemometer for monitoring the outside gas flow conditions. Two different ranges of flow meters were used for measuring flow rates. A Fluke data acquisition system was used for logging the measured data of temperature and flow rates.

The experimental routine was set up for defining a correlation of the medium flow rate vs surface temperature of porous specimens.

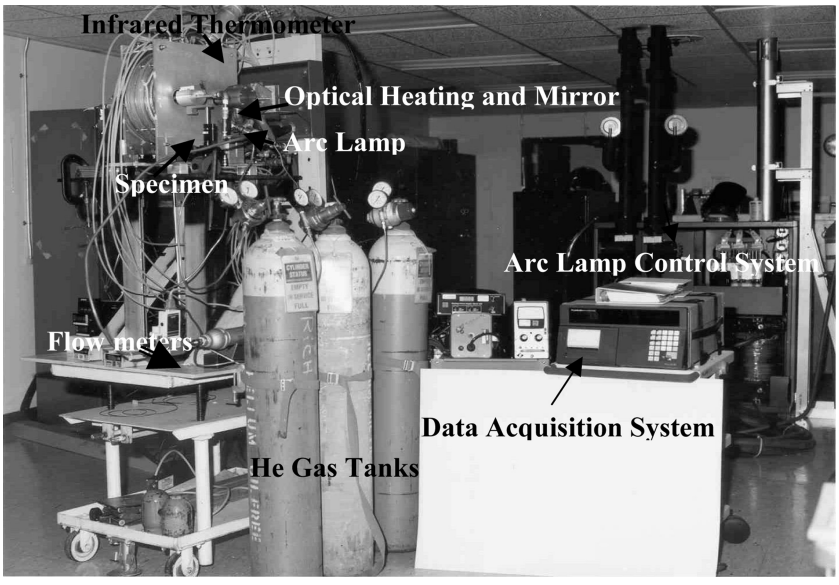

Fig. 4 Experimental setup for transpiration cooling.

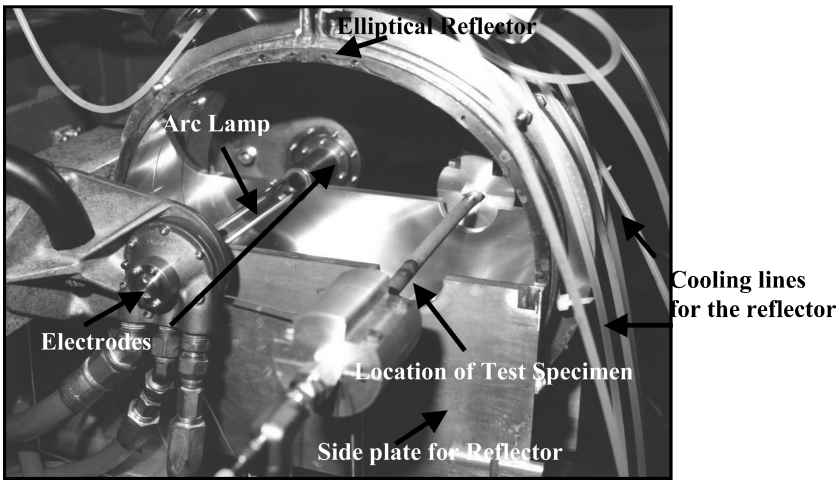

Fig. 5 Optical heater and mirror.

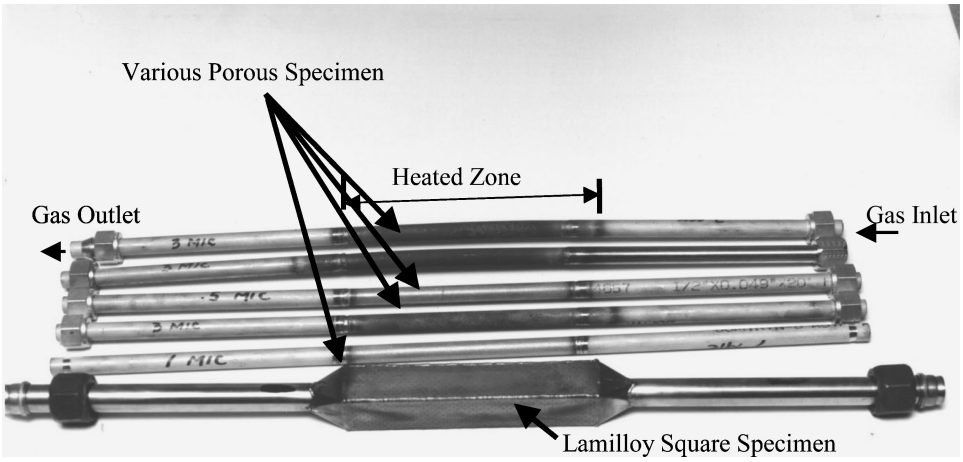

Fig. 6 Typical test specimen for transpiration cooling experiment.

Once the probes and system become operational, helium gas is initially charged into a specimen and allowed to flow through the pores of a specimen before any attempts of heating. Then, the arc lamp was turned on, and its optical beam power was increased step-by-step from a starting point to a final power level to test the responsiveness of heated materials under a constant flow of helium gas. In other cases, the beam power was settled at a level to show an equilibrium point by heat balance while the gas flow rate was varying.

A scramjet is designed to use cryogenic hydrogen as both a propellant and a coolant in its regenerative cycle. In the experiment, room temperature helium gas was used in place of cryogenic liquid hydrogen (LH_2) because the laboratory was not ready to use cryogenic hydrogen. Hence, a compensatory adjustment for heating load was made for the use of room temperature helium. The energy required for heating cryogenic hydrogen to 1000 K is 12,127 $\dot{m}_{H_2}$, but for the room temperature helium, the energy required is 4774 $\dot{m}_{He}$, where the mass flows $\dot{m}_{H_2}$ and $\dot{m}_{He}$ are in grams per square centimeter seconds. Thus, for the same amount of mass flow rate, the experiment with room temperature helium would require a heat flux level of just 234 W/cm^2, rather than the average heat flux, 567 W/cm^2, required for cryogenic hydrogen. Such a scaling conversion for a proportionate heat flux is somewhat complex to obtain because of unknown flow rate of the medium and phase change while transpiring. The maximum heat flux is also determined by the size of a specimen. When the maximum optical power ($\sim$60 kW) of the arc lamp is used for a specimen 2 cm in diameter and 15 cm in length, the irradiance on the specimen surface could reach to approximately 627 W/cm^2, which is more than enough for desired experiment. Under any level of heat flux applied, the specimen was heated and allowed to reach and maintain its temperature without exceeding more than 1000 K by adopting a transpiration cooling mechanism.

Results and Discussion

The first set of specimens used in the experiment was three porous tubes of stainless steel (1.5, 3, and 5 μm in porosity). The other was a porous conduit with a square cross section. The porous wall was built with lamination of thin and perforated stainless-steel plates (Lamilloy[7]). Helium gas was continuously charged into the specimen tube, allowing flow through the porous wall of a specimen while the surface temperature of the specimen was monitored in time. The pressure and flow rates of helium and the heat flux applied were also monitored. Figure 7 shows the surface temperatures of the 3-μm specimen that were measured by the infrared thermometer and thermocouples. The results are shown as a function of helium flow rates.

With one-quarter of the arc lamp's maximum power (60 kW), the outside surface temperature was elevated to 1100°C (1373 K) within 2 min without medium flow. The temperature decreased as helium gas started flowing, increasing as flow rates were increased. However, the inside wall temperature of the specimen dropped rapidly as the flow rates increased, as shown in Fig. 8, because the incoming gas medium at room temperature was quite lower than that of gas blowing out through the porous wall. At low flow rates of transpirant, the cooling rate of the inside surface tended to increase compared with that of the outside surface. This is due to a long, increased dwell time of gas through pores and the low volume of transpirant inside the tube. Increasing transpirant flow rates indicate an increase in

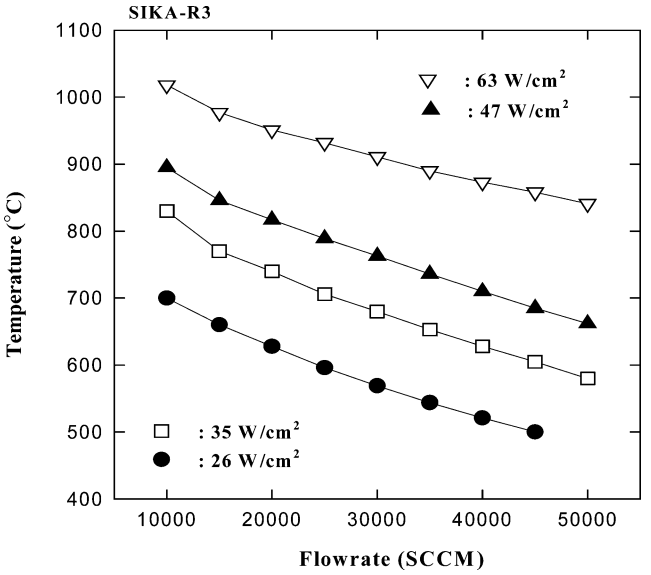

Fig. 7 Outside surface temperatures of sintered tube, 3 μm.

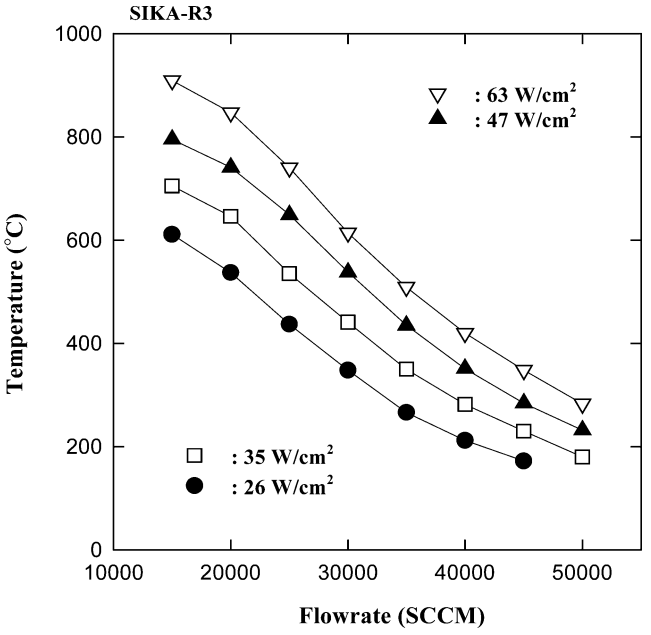

Fig. 8 Inside surface temperatures of sintered tube, 3 μm.

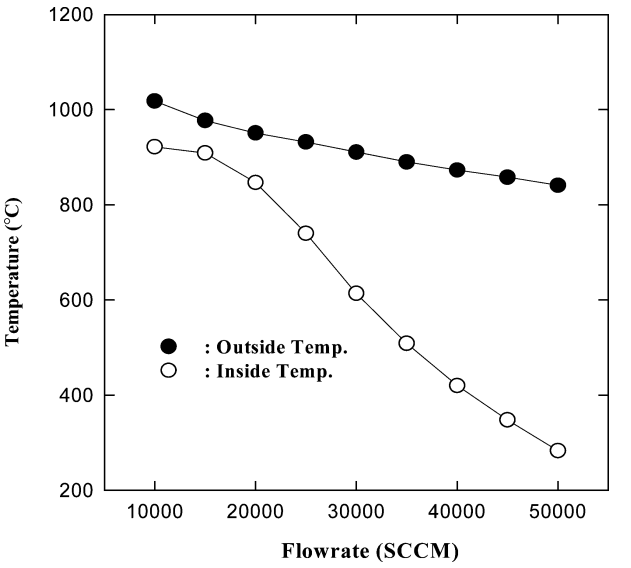

Fig. 9 Temperatures variation of inside and outside surfaces, current 80 A(63 W/cm^2).

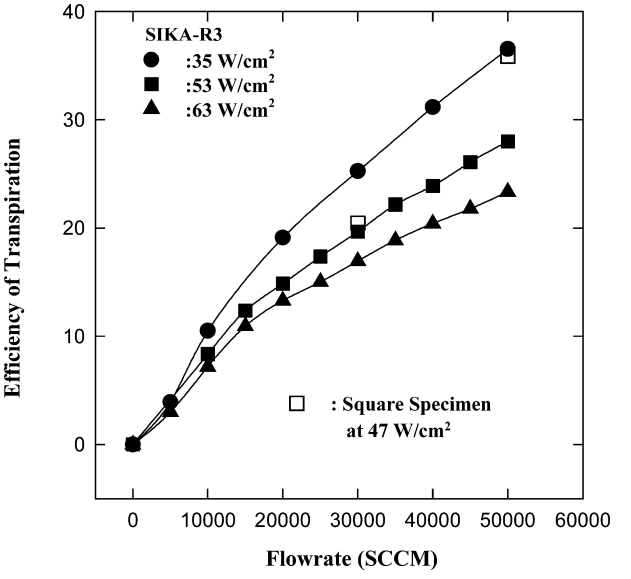

Fig. 10 Efficiency of transpiration, He gas.

the number of gas molecules passing through pores. When the gas accumulates and pressurizes the chamber, propellant gases begin to flow out faster, taking away more heat. However, the conducted heat is still greater than the heat removed by the gas medium until the flow rate reaches a certain point where the inside wall temperature starts dropping. Once the heat removed by transpirant and the heat the inside wall due to conduction establish equilibrium, the inside wall temperature starts dropping with increasing flow rates. This effect causes the temperature of inside surface to drop faster than at the outside surface. The gas medium that goes through a porous wall heats up drastically and becomes less effective for cooling at the outside surface than at the inside surface. As shown in Fig. 9, the outside surface temperature drops gradually even though the flow rates increase. The efficiency of transpiration cooling may be defined as

$$\eta = \frac{T_{g\text{-out}} - T_{g\text{-in}}}{T_s - T_{g\text{-in}}} \tag{1}$$

where, η is the efficiency of the transpiration, $T_{g\text{-in}}$ and $T_{g\text{-out}}$ are the gas temperatures entering and exiting the porous wall, and T_s is the temperature of the specimen at the heated wall. For this study, measurement of the actual gas temperature exiting the specimen porous wall $T_{g\text{-out}}$ could not be easily determined, and so an estimate of relative effectiveness at a given heat flux level was developed as follows.

The difference in gas temperature was estimated by using the heat flux and coolant flow rate as

$$T_{g\text{-out}} - T_{g\text{-in}} \cong \dot{Q}/\dot{m}C_p \tag{2}$$

Where $\dot{Q}$ is the incident heat flux, $\dot{m}$ is the transpirant mass flux, and C_p is the transpirant specific heat capacity. With these quantities known, the cooling effectiveness was obtained by the following approximation:

$$\eta \cong \dot{Q}/[\dot{m}C_p(T_s - T_{g\text{-in}})] \tag{3}$$

The cooling effectiveness by transpiration for both the 3-μm porous and square cross-sectional specimens is shown along with helium flow rates in Fig. 10. The results show that the cooling efficiency increases with flow rate. However, it also shows that for the 3-μm porous specimen, the increment of cooling efficiency with

helium coolant flow rates is slower at a high heating load than at low heating loads. The square cross-sectional specimen with multilayered walls of which each layer has numerous perforated holes for transpiration shows a steep increase in transpiration cooling efficiency as compared with the results of 3-μm porous specimens with increasing flow rates. This is probably due to the difference in the through-the-thickness thermal conductivities of the two specimens.

The multilayered specimen has a very low through-the-thickness thermal conductivity because of spacing between layers. On the other hand, the perforated holes on a thin layer undergo a relatively small change in size or open-hole diameter due to one-dimensional thermal expansion and let a transpirant flow without much alleviation. However, the sintered wall of the 3-μm porous specimen undergoes three-dimensional thermal expansion that reduces the cross-sectional area of flow passage and eventually attributes to slow flow of a transpirant by choking.

When a 234 W/cm^2 heat flux (at the 300 A level of the arc lamp system) was applied, the medium flow through the 3-μm porous specimen was completely choked due to the thermal expansion of the sintered material that eventually blocked the passage of the medium. This phenomenon repeatedly appeared on high heat flux experiments that were carried out with the same test conditions. After chocking, the pressures measured at the flow meters located upstream and downstream were identical at approximately 276 KPa (40 psi). For the squared specimen, the efficiency steeply increased with an increase in flow rate. A history of surface temperature with a uniform flow rate is shown in Fig. 11. The temperature rapidly stabilized within 1 min at 830°C and was very responsive to the flow rate changes. The 5 standard liters per minute (SLPM) change of the flow rates results in a 40°C change in temperature within 6 s. At the constant flow rates (60 SLPM), a time history of the surface temperatures is shown with various heat fluxes from 80 to 117 W/cm^2 in Fig. 11. Figure 12 shows the surface temperature of a square cross section specimen with respect to flow rates under various heat fluxes. The temperature profiles do not show equilibrium temperatures corresponding to heat fluxes. However, under the heat fluxes of 130 and 150 W/cm^2, the surface temperature profiles show a tendency that would reach equilibrium temperature if the flow rates continued to increase. Because the maximum flow rates of helium was limited to 500 SLPM in the experiments, the profiles in Fig. 12 could not show the equilibrium points.

It is important to show and estimate the performance for a case in which hydrogen is used instead of helium, because the scramjet actually uses cryogenic LH_2. To compare the estimated result to the tested data of helium, hydrogen gas at a room temperature rather than cryogenic LH_2 was used. The transpiration cooling performance of hydrogen gas that was evaluated by the use of the test results and

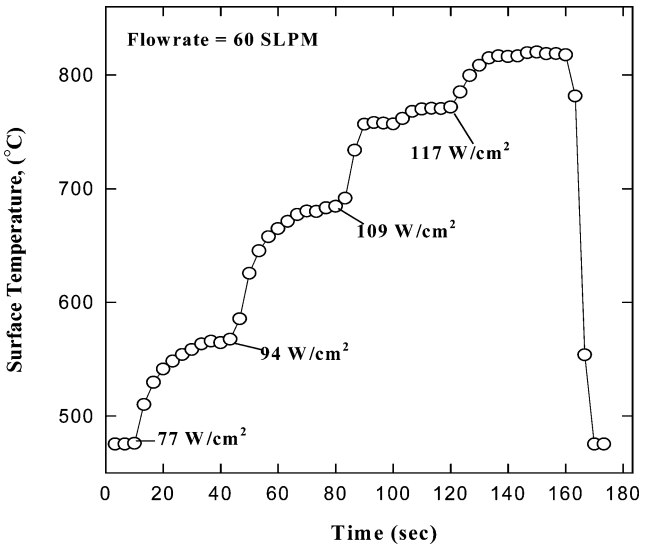

Fig. 11 Surface temperatures corresponding to various heat fluxes at fixed flow rates.

Table 1 Parameters of gaseous transpirants

Gas	C_p, cal/g · C	μ, m^2/Darcy[a]	κ, Darcy
He	1.25	471.3×10^{-7}	0.001
H_2	4.08	213×10^{-7}	0.001

[a]Darcy $= 0.987 \times 10^{-6}$ m^2.

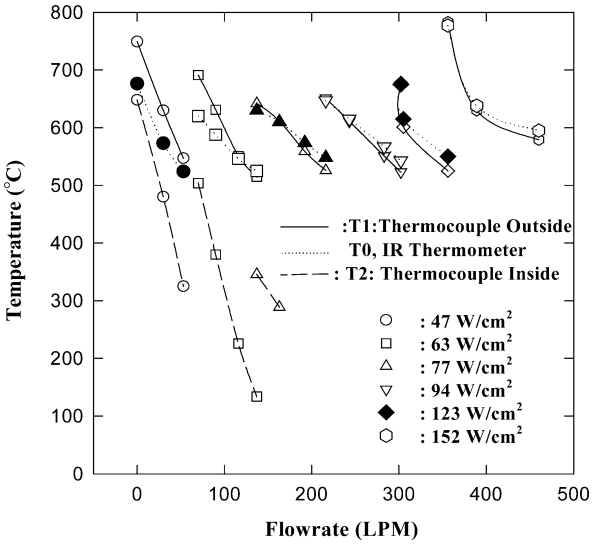

Fig. 12 Surface temperatures of squared cross-sectional tube.

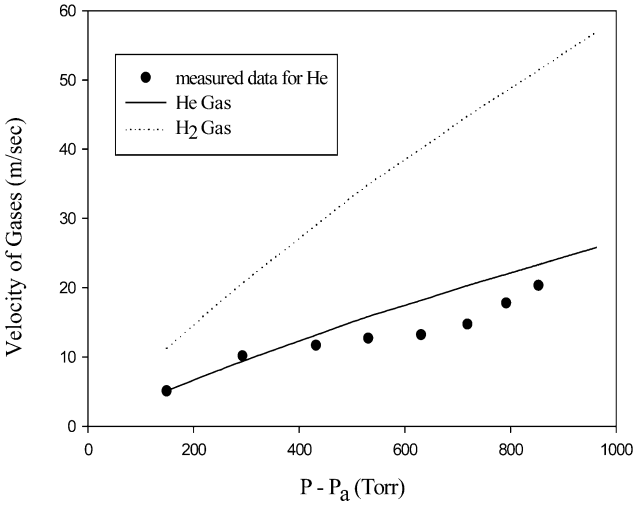

Fig. 13 Velocities of He and H_2 gases through porous media.

thermophysical properties of helium transpirant would reveal how the use of helium in the experiment is justified and helps guess the performance for a case when cryogenic LH_2 is used as a transpirant. The conversion was made on the basis of test parameters of helium transpirant and according to the scaling factors of thermo-physical properties of hydrogen as opposed to those of helium. The Darcy equation for a flow of gas through a porous media is described as

$$V = -C(\kappa/\mu)\left[\left(P^2 - P_a^2\right)/2Pt\right] \tag{4}$$

in centimeters per second, where C is a conversion constant (1.333×10^4), κ is the permeability of the material in square meters, μ the viscosity in kilograms per meter second, t the thickness in centimeters of the porous material, and P and P_a the pressures in torr inside and outside the porous media, respectively. Nominal values for the specific heat, permeability κ and viscosity μ are listed in Table 1. Using the Darcy equation, the velocities of the helium and hydrogen are calculated and shown in Fig. 13 along with measured

data derived from the flow meter. The result shows that the velocities of the two gases were not linearly changed for the differential pressure. The thermophysical properties of gases through a porous medium, such as thermal conductivity, specific heat, viscosity, and diffusivity, in terms of the gas temperatures, were evaluated with the data that were available in Ref. 8 and the results from the experimental data. The thermal conductivities of He and H_2 were quite linear with gas temperature from 300 to 1500 K (Fig. 14). Figure 15 shows that the differential pressures of the helium and hydrogen gases are increased with the gas flow rates.

The energy absorbed by the transpiration of H_2 can be estimated from H_2 data by assuming that the effectiveness for the two gases is similar. For a porous specimen, the heat balance can be formulated as

$$\dot{Q}_{\text{in}} = \dot{Q}_{\text{conv}} + \dot{Q}_{\text{rad}} + \dot{Q}_{\text{cond}} \tag{5}$$

where $\dot{Q}_{\text{in}}$ is the input power, $\dot{Q}_{\text{cond}}$ the conduction loss through the specimen ends, Q_{conv} the convective heat loss of the transpirant, and $\dot{Q}_{\text{rad}}$ the radiative loss. It was implicitly assumed that $\dot{Q}_{\text{cond}}$ and $\dot{Q}_{\text{rad}}$ were small enough to be negligible. To provide an indication of the relative capabilities of He and H_2 to absorb heat in transpiration process, the effectiveness is assumed to be unity for both coolants in the following equation. Then, $\dot{Q}_{\text{conv}}$ can be written as

$$\dot{Q}_{\text{conv}} = A_s C_p \dot{m} (T_s - T_{g\text{-in}}) \tag{6}$$

where A_s is the heated area of a specimen. By the use of the Eq. (6) with the appropriate values for C_p, the experimental results for He cooling, and the scaled calculation of H_2 mass flow rate described earlier, the convective heat removal rates $\dot{Q}_{\text{conv}}$ for the two gases are shown in Fig. 16. This result indicates that the transpiration cooling effects by hydrogen gas far exceed those attainable by using helium.

The performance comparison between a circular porous tube and a perforated, square cross-sectional tube are further illustrated in Figs. 17 and 18. To maintain the surface temperature around 600°C for a heat flux of 152 W/cm^2, the flow rates required for a circular porous tube was 75 SLPM after a projected run (750 s). For the squared cross-sectional tube, a 500-SLPM flow rate was required to maintain the temperature. These results reflect the large differences in through-the-thickness thermal conductivities, the effective porosity differences, pore sizes, and geometrical differences between these two specimens tested under a similar condition setting. In general, the temperature drops shown as the valleys correspond to the flow rate increases for both specimens. As the heat flux increases,

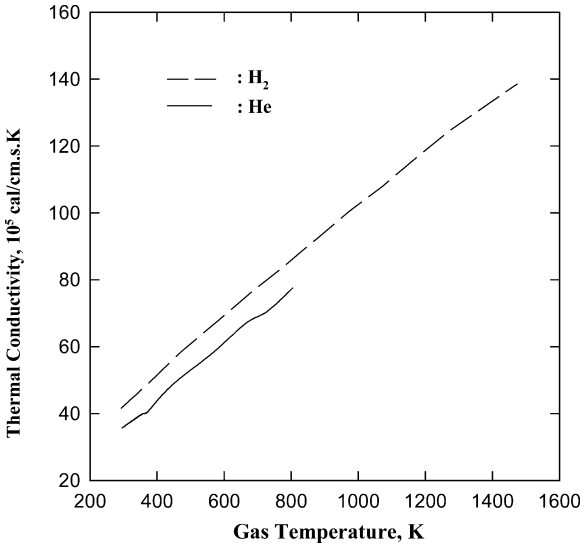

Fig. 14 Thermal conductivities of helium and hydrogen.[8]

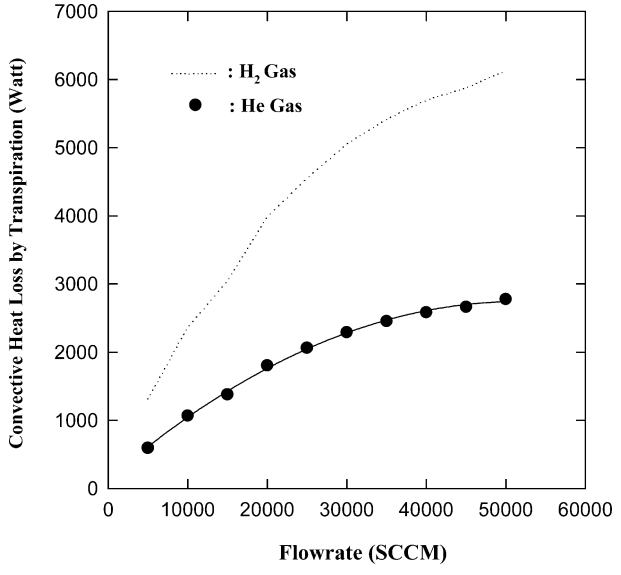

Fig. 15 Temperature variation of inside and outside surfaces.

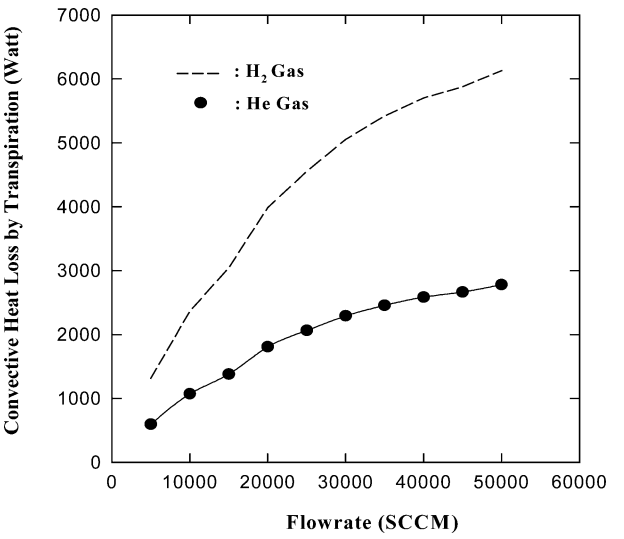

Fig. 16 Convective heat absorption capability as function of He and H_2 gas flow rates for porous tube specimen.

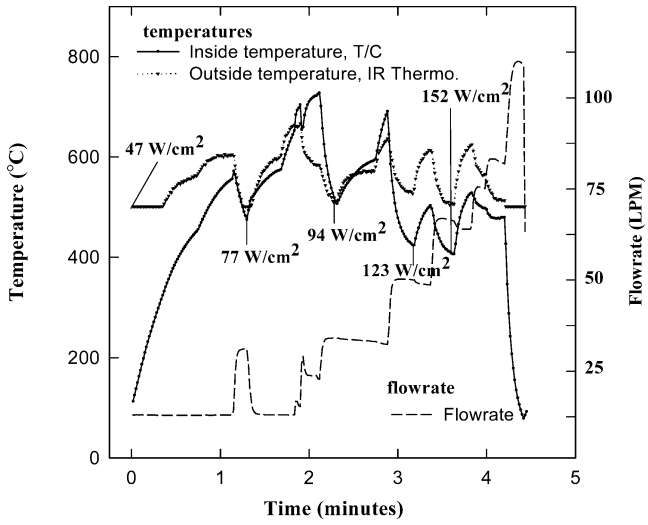

Fig. 17 Temperature responses of 3-μm circular porous tube with respect to heating loads and helium flow rates.

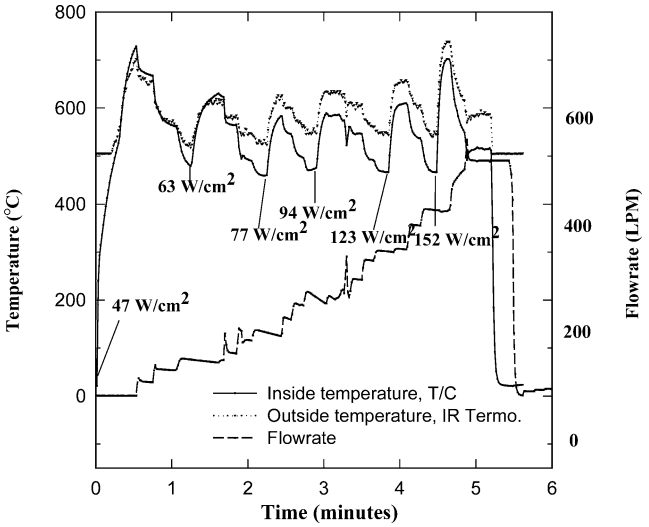

Fig. 18 Temperature responses of square cross-sectional tube with respect to heating loads and helium flow rates.

the temperatures increase too, for both specimens. Strangely, there are some irregularities in the temperature profiles for the inside and outside surfaces of a circular porous tube specimen as shown in Fig. 17. For some cases, the inside temperatures were higher than the outside temperatures. Following the temperature profiles closely, one may find that the spikes distinctively respond to the flow rates. This is probably because a change in pore structures of a sintered body or an unsecured thermocouple attachment to the inside surface by thermal expansion becomes a dominant factor that causes this phenomenon when a flow of transpirant becomes steady.

Conclusions

A study of transpiration cooling for scramjet combustors was performed with various specimens using an optical heating method. The optical heating offered the benefit of applying heat to a specimen without affecting or altering the transpirant flow rate and boundary layer. It is found that the surface temperatures responded rapidly to the heat fluxes and the flow rates. Also, significant temperature gradients through the thickness of a specimen were observed at the higher heat fluxes and the higher flow rates. One of the distinctive effects observed through the experiments was the choking effect that blocks the flow passage of transpirant through a porous wall due to the reduced flow channel cross section by thermal expansion. The choking effect was so significant for the 3-μm sintered specimens that the overall flow was terminated at one point when a 234 kw/cm^2 heat flux was applied. Such an effect was not noticed from the square cross-sectional specimen, which was fabricated with multilayers of sheet metal with perforated holes, at any heat flux levels.

The results of a scaling conversion study to estimate thermal performance when hydrogen is used in place of helium show that hydrogen has a much higher cooling capacity compared with helium because hydrogen has a similar thermal conductivity, higher specific heat, and higher flow velocity due to its small atomic cross section and low viscosity. In real scramjet applications where cryogenic LH_2 is available, the more efficient cooling by hydrogen transpirant would allow much higher heat flux handling capability than that determined using helium in the experiment.

Acknowledgments

This work was partially supported by the NASA Langley Research Center Grant NAG-1-1513.

References

[1]Kelly, H. N., and Blosser, M. L., "Active Cooling from the Sixties to NASP," NASA TM 109079, July 1994.

[2]Raghuraman, P., Anderson, B. J., Sieger, S. N., Rousar, D. C., Hidahl, J. W., Baxer, K. E., "The HEDI Platelet Transportation Cooling Concept—Light Weight, Durable, Flight Proven," AIAA Paper 94-2005, May 1994.

[3]Zhang, H. J., and Zhao, X. B., "Critical Heat Flux for Thin Powder Porous Layer," Experimental Heat Transfer, Fluid Mechanics, and Thermodynamics, Elsevier Science Publ. Co., Inc., Dubrovnik, Yugoslavia, 1991, pp. 627–632.

[4]Hadim, A., and Burmeister, L. C., "Onset of Convection in a Porous Medium with Internal Heat Generation and Downward Flow," *Journal of Thermophysics and Heat Transfer*, Vol. 2, No. 4, 1988, pp. 343–351.

[5]Masuzawa, J., Tanahashi, T., and Ando, T., "Flow Entrance Region in a Porous Pipe," *Bulletin of the Japan Society of Mechanical Engineers*, Vol. 23, No. 179, 1980, pp. 672–678.

[6]Porous Stainless-Steel Tube SIKA-R3, Newmet Krebsoge, Inc., Terryville, CT.

[7]Lamilloy, Allison Gas Turbine Div., General Motors Corp., Indianapolis, IN.

[8]*Handbook of Heat Transfer*, McGraw–Hill, New York, 1975, Sec. 2, pp. 2–88.